

Prospects for 4-laser white-light sources

Snjezana Soltic & Andrew N. Chalmers

To cite this article: Snjezana Soltic & Andrew N. Chalmers (2019) Prospects for 4-laser white-light sources, Journal of Modern Optics, 66:3, 271-280, DOI: [10.1080/09500340.2018.1517904](https://doi.org/10.1080/09500340.2018.1517904)

To link to this article: <https://doi.org/10.1080/09500340.2018.1517904>



© 2018 The Author(s). Published by Informa UK Limited, trading as Taylor & Francis Group.



Published online: 11 Sep 2018.



Submit your article to this journal [↗](#)



Article views: 634



View related articles [↗](#)



View Crossmark data [↗](#)

Prospects for 4-laser white-light sources

Snjezana Soltic^a and Andrew N. Chalmers^b

^aSchool of Professional Engineering, Manukau Institute of Technology, Auckland, New Zealand; ^bInstitute of Biomedical Technologies, Auckland University of Technology, Auckland, New Zealand

ABSTRACT

This paper describes a series of simulation experiments designed to demonstrate the feasibility of using solid-state lasers in white-light mixtures. The mixed-laser sources are evaluated in terms of the luminous efficacy of the radiation (LER) as well as different measures of colour performance. The latter include the CIE colour rendering index (R_a) and the IES colour fidelity index (R_f) as well as a selection of additional parameters in the two systems. Optimization of the mixtures is achieved by the use of purpose-designed differential evolution algorithms. The best results to date (with four real laser wavelengths) are R_f of 84 with LER 364 lm/W, which indicate the feasibility of the mixed-laser approach to provide highly efficient, energy-saving light sources. These prospects will be further enhanced by potential future developments in semiconductor lasers, with the possibility of producing R_f of 86 with LER of 380 lm/W.

ARTICLE HISTORY

Received 8 March 2018
Accepted 17 August 2018

KEYWORDS

Semiconductor lasers; spectral design; differential evolution; white light; colour rendition; luminous efficacy of radiation

Introduction

It is the intention of this paper to introduce the concept of white-light laser mixtures for general-purpose illumination, and to alert the laser community to the possibilities of developing lasers with appropriate properties for use within light sources.

A brief lighting background


The spectral design of any light source needs to take account of two important lighting attributes, termed luminous efficacy and colour rendering, which are in general contravariant. It is possible, however, by careful spectral design of any light source, to achieve an optimum combination of these features, and this is an additional objective of this paper.

Colour rendering has been defined by the CIE (*Commission Internationale de l'Éclairage*, International Commission on Illumination) who have published recommendations for the method of calculation of their CRI (colour rendering index) (1) based on a knowledge of the light-source spectrum. As of the time of writing, this is the internationally agreed method. Note that CRI and associated technology has also been covered in (2). The two most widely-quoted colour rendering terms are: R_a – the general colour rendering index, based on the colour shifts (caused by the test source) of eight

moderate-chroma colour samples; and R_9 – the ‘special’ (individual) index for the highly saturated red colour (sample 9 in the CIE system).

In order to remove some of the inconsistencies inherent in the CIE CRI method, and to update the methods of calculation, the NIST in 2010 proposed (3) their CQS (colour quality scale). The method is again based on the colour-shift principle – but now using 15 high-chroma test colour samples. There are several innovative refinements that aid in assessing colour quality, giving the general colour quality index Q_a as output. An alternative calculation gives the colour fidelity index Q_f which is intended to be an alternative to R_a .

Some dissatisfaction with the above two methods has arisen since the widespread adoption of LED (light-emitting diode) lighting. As a consequence, the IES (Illumination Engineering Society of North America) has adopted a recommended method (TM–30–15) (4,5) which recommends two new indices (R_f and R_g) for the classification of the colour properties of light sources. The underpinning research leading to the development of TM–30–15 (5–7) identified weaknesses in both the earlier methods (1,3), claiming that they do not adequately sample wavelength space and hence tend to over-estimate colour performance. The new IES index R_f gives an overall assessment of colour fidelity, while gamut index R_g indicates the relative magnitudes of colour shifts for sample colours in different regions of colour space.

CONTACT Snjezana Soltic  ssoltic@manukau.ac.nz
https://protect-us.mimecast.com/s/_UhCL9YPoHRMMX36CqkKgV?domain=docs.google.com

© 2018 The Author(s). Published by Informa UK Limited, trading as Taylor & Francis Group
This is an Open Access article distributed under the terms of the Creative Commons Attribution-NonCommercial-NoDerivatives License (<http://creativecommons.org/licenses/by-nc-nd/4.0/>), which permits non-commercial re-use, distribution, and reproduction in any medium, provided the original work is properly cited, and is not altered, transformed, or built upon in any way

In this paper we refer to the CIE R_a method and the IES R_f method, since the CIE R_a is still at this time the internationally used metric for colour rendering, and the IES R_f is believed to offer a more exacting assessment of the colour performance of the white light produced by laser mixtures.

The LER (luminous efficacy of the radiation) of a light source assesses the ‘lighting content’ of the spectrum by comparing the visible light output (in lumens) against the total radiant output (in watts) as in Equation (1)¹.

$$\text{LER} = \frac{K_m \int_{\lambda} V(\lambda) S(\lambda) d\lambda}{\int_{\lambda} S(\lambda) d\lambda} \quad (1)$$

where K_m is the maximum luminous efficacy of radiation (≈ 683 lumen per watt), $S(\lambda)$ is the spectral distribution of the light source and $V(\lambda)$ is the CIE spectral sensitivity function for photopic vision (8).

It is common for lighting designers to select light sources for specific tasks by reference to the source CCT (correlated colour temperature) since this serves as an indication of the colour of the source and the ‘atmosphere’ that it will create. The CCT is defined in (9), and is directly linked with the CIE chromaticity of the source, which may be expressed in terms of any one of the following pairs of chromaticity coordinates, namely (x, y) ; (u, v) ; or (u', v') , which are all linearly related to the CIE (X, Y, Z) tristimulus values². Note that it is possible for many different SPDs (spectral power distributions) to have the same CCT; and that CCT is not essentially linked with colour rendering or fidelity.

The (u', v') coordinates are classed as providing a uniform chromaticity scale and are used in most modern light-source specifications. Hence, in this paper we use the (u', v') coordinates, in addition to the CCT, to define the chromaticity of each source we simulate.

Lasers in lighting

It has previously been shown (10) that it is possible to produce white light mixtures optimized to achieve good-to-excellent CRI (colour rendering index) together with high values of LER (luminous efficacy of radiation) by the use of at least four laser wavelengths. These optimizations were unconstrained, in that any four wavelengths could be derived that met the optimization criteria. Hence, a shortcoming of the work was that the optimizations were of little value unless the lasers actually existed to provide the relevant wavelengths. A further criticism relates to the claimed under-sampling of wavelength space in the CIE method (5–7); and it has been stated that ‘the concept of an optimized line spectrum appears to be due to a failure of the CRI methodology rather than to an actual optimization of colour rendering properties’ (11).

In other words, the previous mixed-laser optimizations based on CRI would be invalidated, and hence proposals for white light mixtures of lasers negated, since there will always be some surface colours that are inadequately rendered by such discontinuous spectra. We cannot deny the facts underlying such assertions; however we take the view that there will still be a place for mixed laser sources in future lighting systems where there may be a demand for high (overall) luminous efficacies, as long as steps are taken to maximize their TM–30–15 performance.

The purposes of this paper are thus twofold: 1, to find laser combinations that have acceptable-to-good (even if not the highest) colour performance, and 2, to attempt to find mixtures of real lasers that are able to satisfy these criteria. In pursuit of objective 1, we harness the tools of the TM–30–15 method to re-assess earlier optimizations, while also creating new optimization tools based on that method. One such tool is described in this paper that will satisfy objective 2 by optimizing mixtures of real lasers.

Topics covered in subsequent sections of this paper will include:

- Lasers as light sources, and current real-laser wavelengths.
- Re-assessment of earlier work, and how well the CRI-optimized mixtures perform in the light of TM–30–15.
- Unconstrained R_f optimizations.
- R_f optimizations of real laser mixtures.

Lasers as white sources

Table 1 gives a brief overview of the two main types of laser lighting currently under development.

It was shown in (10) that there is no LER penalty for narrow line-widths in the spectrum of a light source, and we will show that LER values in excess of 350 lm/W are achievable for white-light combinations of four 1-nm bands. It is anticipated that lasers will be able to achieve this performance without the lumen-output ‘droop’ that is characteristic of LEDs. The key benefit of semiconductor lasers as sources is likely to be the high conversion efficiency (radiant-to-electric power ratio) potentially attainable at high current densities. Although variable, depending on the specific wavelengths, lasers of the near future should equal or outstrip the conversion efficiencies of available LEDs. These factors must make lasers the contenders to be the highest-power, highest LER sources in the future lighting scenario (12–14).

It is also evident that considerable research is being put into the development of laser-phosphor combinations as white light sources (15). The benefits of this lie

Table 1. Summary of types and properties of laser sources.

Laser-Diode Light Sources		
	Phosphor converted	Direct (optimized) mixtures
Pros	<ul style="list-style-type: none"> • Wideband phosphor output – can give better colour rendition • Simpler electronics – single diode to be controlled • Incoherent phosphor output assists de-speckling • Simpler thermal control with the single diode 	<ul style="list-style-type: none"> • Optimized mixture gives generally-acceptable colour rendition • High LER from optimized mixtures • Higher total lumen output of package
Cons	<ul style="list-style-type: none"> • Choice of phosphors critical for good colour rendition • Limited quantum efficiencies of phosphors – hence lower LER • Total lumen output of package likely to be more limited 	<ul style="list-style-type: none"> • Line spectrum provides reduced but useful colour rendition • More complex electronics – 4 diodes to be controlled • De-speckling and de-cohering optics required • More complex thermal control with multiple diodes.

in the improvements in colour rendering (and colour fidelity) attainable with the broader bandwidths generally delivered by phosphors. However, as Coltrin et al. (12) have pointed out, there are Stokes-shift and quantum-efficiency losses in each phosphor, and these will reduce the overall efficiency (and hence also efficacy) by significant margins.

We have therefore taken the approach of working with the direct laser outputs in the mixtures discussed in this paper. For simplicity in our predictions and simulations, we assume throughout that each laser output has a bandwidth of 1 nm (which, from the colour rendering perspective, leads to worst-case estimation).

Real laser mixtures

In order to find optimized mixtures of real lasers as white light sources, we created a database of 57 lasers having outputs between 400 and 780 nm – based on a search of the online catalogues of several suppliers of visible-light semiconductor lasers. A number of the selected products have been identified as DPSS (Diode pumped solid state) lasers. In these devices the output is obtained indirectly by diode-pumping of a separate laser crystal, sometimes also using frequency doubling or other heterodyning principles, and the efficiency will be reduced as a consequence of losses in such systems (16). Unfortunately we have had difficulty in clearly identifying exactly which of our 57 units operate on DPSS principles, and many are sold simply as ‘Plug and play benchtop lasers’.

At this stage we are not attempting to isolate only the ‘pure’ laser diodes. However, if any of our identified

(optimized) laser wavelengths turn out to be available only in DPSS devices, we would urge laser manufacturers to look into ways of designing laser diodes that can deliver these wavelengths directly. This will be particularly important if lighting manufacturers are to realize the energy-saving benefits of lasers as future light sources.

A previous example

One example of a real laser mixture has been noted in (10) and refers to an experiment by Neumann et al. (13) in which 4 solid state lasers were used in different combinations to provide CCT values of 5665, 4256, 3111, and 2838 K. The wavelengths were 457, 532, 589, and 635 nm.

In order to determine the TM-30-15 properties of these mixtures, we have simulated them using 1-nm bandwidth (pseudo) delta-functions at the above-mentioned wavelengths, and have calculated their intensities from the data of Table 1 in (13). Our results are shown here in Tables 2 and 3.

Comparing the target results with those achieved by simulation, the average absolute differences were as follows. Colour rendering measures, from Table 2: $\Delta R_{a(ave)} = 0.0$; $\Delta R_{9(ave)} = 2.3$. Average differences in source colorimetry data, from Table 3: $\Delta CCT^{-1} = 2.02 \text{ MK}^{-1}$; $\Delta E'_{uv} = 0.001$. Note that colour temperature differences are conveniently represented in reciprocal-megakelvin differences (also known as ‘mired’ or ‘micro-reciprocal-degrees’)³, calculated using Equation (2).

$$\Delta CCT^{-1} = \frac{1}{CCT_a} - \frac{1}{CCT_b} \quad (2)$$

The chromaticity differences are computed from the (u' , v') chromaticity coordinates using Equation (3).

$$\Delta E'_{uv} = \sqrt{(u'_a - u'_b)^2 + (v'_a - v'_b)^2} \quad (3)$$

where the subscripts a and b in these two equations refer respectively to the two light sources being compared.

It is evident that there is close correlation of the simulated results for R_a , R_9 , chromaticity and CCT with those quoted in (13), and we conclude that we have achieved good estimates of the original spectra for the 4 different CCTs quoted in their paper. Neumann et al. also conducted a number of carefully-controlled visual assessments of their laser mixtures in comparison with suitable reference sources (with matched colour appearance). The following is a very brief summary.

A pair of side-by-side viewing booths was set up, and they were provided with identical bowls containing natural fruit and wrapped candy, placed at the bottom centre of each viewing booth, serving as coloured test objects.

Table 2. Simulation of the spectra formulated by Neumann et al. (13).

	Targets*			Simulations – based on data in Table 1 of Neumann paper									i_{min} Sample No.
	CCT		R_9	CCT		LER		R_f	R_g	R_{fskin}	R_{fmin}		
	kelvin	R_a		kelvin	lumen per watt	R_a	R_9						
Cool White	5665	83	82	5564	349	83	84	76	105	90	20	75	
Neutral White	4256	85	75	4217	333	85	71	78	109	93	27	42	
Warm White	3111	90	95	3130	357	90	93	82	108	92	37	42	
Incan-descent	2838	91	96	2844	355	91	95	82	108	92	38	42	

*Targets are the results achieved by Neumann et al. (13).

R_a and R_9 are defined in CIE 13.3–1995 (7).

R_f , R_g , and R_{fskin} are defined in TM–30–15; R_{fmin} and i_{min} are deduced from TM–30–15 (17).

Table 3. Colorimetric data for the Target and Simulated spectra.

Source	Target colour			Simulated source colour			ΔCCT^{-1} (MK ⁻¹)	$\Delta u'$	$\Delta v'$	$\Delta E'_{uv}$
	CCT (K)	u'	v'	CCT (K)	u'	v'				
Cool White	5665	0.197	0.486	5564	0.198	0.487	3.20	0.001	0.001	0.002
Neutral White	4256	0.224	0.490	4217	0.226	0.489	2.17	0.002	0.001	0.002
Warm White	3111	0.246	0.521	3130	0.246	0.521	1.95	0.000	0.000	0.000
Incandescent	2838	0.256	0.526	2844	0.256	0.526	0.74	0.000	0.000	0.000
Average Differences							2.02	0.001	0.001	0.001

Magnitudes only are shown for the differences (ΔCCT , $\Delta u'$, $\Delta v'$, $\Delta E'_{uv}$).

Comparisons were carried out by a number of colour-normal volunteers. Illuminances were in the 125–200 lux range. Some systematic deviations were noted among the viewers' responses, but there was nevertheless a general conclusion that 'in terms of colour rendering quality, the laser illuminant is nearly indistinguishable from high-quality reference illuminants' (13).

Our conclusion is that laser mixtures having R_f values in the approximate range of 76 to 82 gave acceptable rendering of the colours of fruit samples and printed candy wrappers – and this indicates an acceptance of the illumination from discontinuous spectra for general lighting purposes. In order to allow for possible tolerances in the above figures, and for the relatively low lighting level in the (13) experiment, we will aim in our work for the optimization of simulated laser spectra having $R_f \geq 84$.

Differential evolution

The optimization process utilizes a differential evolution algorithm and operates within Matlab® under the control of a purpose-built user interface. The features of our optimization tool have been described elsewhere (10,18) but are briefly reviewed here for purposes of completeness. The optimizer operates to derive a light-source spectrum having the 'best' qualities according to a defined performance criterion (or, fitness function). It can be set to work from a specific library of SPDs (here termed 'constrained optimization') or, alternatively, to freely assemble a 'desirable' SPD (as determined by the fitness function) in an 'unconstrained optimization' mode. In attempting to tackle the optimization problem from

several directions, we have adopted both unconstrained and constrained approaches. The unconstrained mode is usually able to deliver 'better' spectra with more desirable properties, but has the disadvantage that the SPD may be difficult or impossible to realize in practice. The constrained mode allows one to define a library of real SPDs with which the optimizer can work, so that the results are realizable in practice; however, the performance of the resulting spectrum may be reduced.

In the present work we have simulated the spectrum of each laser as a single (pseudo) delta-function of 1 nm bandwidth located at the centre wavelength of its output. It is recognized that this is an approximation since real semiconductor lasers typically have a spectral bandwidth of 2 nm or greater. We regard our approximation as providing a worst-case estimate since, in most circumstances, a broadening of the spectrum leads to slight improvements in colour performance.

Unconstrained optimisations

The first phase of this new work was to determine the IES TM–30 properties of a number of optimized 4-laser mixtures derived using the method described in (10). The decision to focus only on 4-laser mixtures in the present work is based on the greater complexity in practice of 5- and 6-laser mixtures (and 3-laser mixtures are ruled out because of their generally poorer colour properties).

Optimizing with CIE 13.3

This experiment followed the method described in (10), in which the fitness function was defined as in

Table 4. Optimization in terms of CIE 13.3.

SPD number	Wavelengths nanometres				CCT kelvin	CIE (u', v') co-ord's	LER lumen per watt	CIE 13.3		TM-30-15			
								R_a	R_9	R_f	R_{fskin}	R_{fmin}	i_{min}
3.1	<u>445</u>	504	557	617	4718	0.204, 0.507	354	92	91	84	92	37	81
3.2	<u>447</u>	502	555	615	4310	0.216, 0.503	353	92	87	85	88	36	81
3.3	448	509	563	618	3945	0.221, 0.513	368	93	94	85	97	34	81
3.4	<u>445</u>	504	558	617	3804	0.220, 0.526	375	93	94	83	90	23	81
3.5	<u>445</u>	509	564	620	3780	0.223, 0.522	372	92	79	85	98	33	81
3.6	452	508	564	618	3604	0.230, 0.517	373	93	86	85	93	25	81
3.7	450	508	562	619	2906	0.253, 0.528	378	95	89	85	94	22	81
3.8	453	<u>510</u>	564	619	2902	0.252, 0.533	386	95	91	85	92	19	81

TM-30-15 parameters are calculated after optimization.
 Gamut index: $97 \leq R_g \leq 103$.
 Underlined wavelengths are available in real semiconductor lasers.

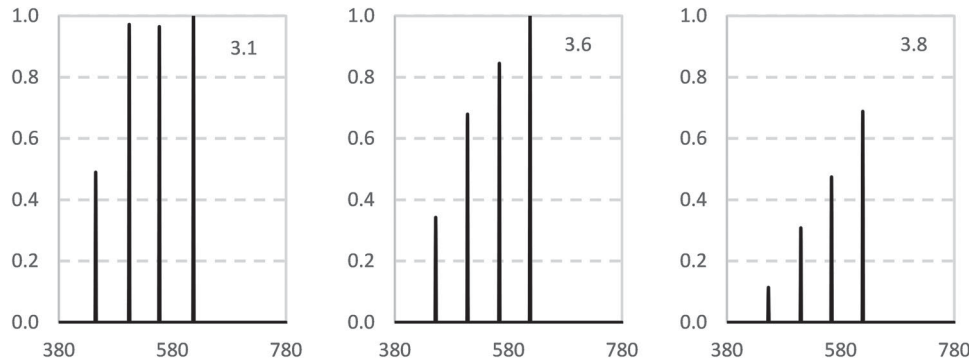


Figure 1. Relative spectral power distributions versus wavelengths (nm) for three of the Table 4 optimized spectra (identified by the SPD numbers in Table 4).

Equation (4):

$$f_1 = aR_a + bR_b + cR_c + dR_{min} + e\eta \quad (4)$$

where the user-selected weighting factors a, b, c, d , and e (any real numbers) control the influence of the parameters R_a, R_b, R_c, R_{min} and η respectively on the optimization of the mixture. Note that:

R_a = CIE colour rendering index, using the first 8 test colours defined in CIE 13.3

R_b = similar to R_a , but for the 6 additional test colours in CIE 13.3

R_c = similar to R_a , but for all 14 test colours in CIE 13.3

R_{min} = the lowest value of R_i for $i = 1 \dots 14$ as defined in CIE 13.3

η = LER (luminous efficacy of the radiation) in lm/W.

In addition: R_9 = the value of R_i for $i = 9$ (saturated red sample in CIE 13.3).

In a series of 30 new tests, we optimized for R_a , etc, and then used the IES TM-30-15 calculation tool (17) to find the IES parameters of each resulting SPD. By careful choice of the weighting factors, we achieved eight SPD results that yielded CCT > 2800 K plus $R_a > 90$, together with $R_f \geq 83$ (with $R_f = 85$ in six cases). They are listed in Table 4 in descending order of CCT. Figure 1 shows the SPDs for three of the listed results, identified by the SPD numbers in the table.

Note that all the TM-30-15 results were calculated after completion of the optimizations. The TM-30-15 parameters used here are as follows:

R_f = IES colour fidelity index, as defined in TM-30-15

R_{fskin} = IES skin rendition index (average of CES15 and CES18 in TM-30-15)

R_{fmin} = the lowest value of R_{fi} for $i = 1 \dots 99$ in TM-30-15

i_{min} = the sample (CES number) giving R_{fmin}

Not listed here is the IES TM-30-15 gamut index, R_g . Note that the R_g values for the eight spectra listed above were between 97 and 103. The wavelengths in the eight SPDs are reasonably tightly clustered around the average values, i.e. 448, 507, 561, 618 nm. However, of the 32 individual wavelengths required in these mixtures, we have found only 4 that exist in currently-available solid-state lasers (445, 447, 450, and 510 nm, with a total of 6 occurrences).

In reviewing the above results (with the exception of SPD 3.5) it is clear that, with $R_a \geq 92$ and $R_9 \geq 86$, these would be regarded in terms of CIE 13.3 as excellent CRI performers. Bearing in mind the previously mentioned caveats (7,11), we have computed the IES TM-30-15 performance data, and found the creditable results of $R_f \geq 83$, $R_g \geq 97$ and $R_{fskin} \geq 88$. However, these need to be balanced against the low values of R_{fmin}

Table 5. Unconstrained optimizations in TM–30–15. (Representative results for ten spectra having $R_f = 85$ or 86).

SPD number	Wavelengths nanometres				CCT kelvin	CIE (u', v') co-ord's	LER lumen per watt	TM–30–15				CIE 13.3	
								R_f	$R_{f_{skin}}$	$R_{f_{min}}$	i_{min}	R_a	R_g
4.1	449	508	564	626	5520	0.198, 0.490	327	86	96	62	98	85	12
4.2	449	512	565	625	4259	0.211, 0.516	365	85	95	60	81	84	36
4.3	451	517	571	628	3890	0.219, 0.524	368	85	92	64	81	83	32
4.4	451	<u>510</u>	565	623	3401	0.234, 0.525	368	86	91	39	81	90	42
4.5	451	<u>515</u>	572	630	3379	0.234, 0.529	359	85	91	57	37	83	24
4.6	453	<u>515</u>	571	629	3203	0.240, 0.530	359	86	90	59	97	84	18
4.7	453	<u>520</u>	570	627	3194	0.240, 0.532	373	85	90	64	81	84	13
4.8	451	516	568	626	3156	0.240, 0.538	380	86	91	54	81	85	28
4.9	455	524	<u>577</u>	628	2955	0.248, 0.540	383	85	88	60	42	87	55
4.10	456	<u>525</u>	580	630	2866	0.253, 0.535	372	85	88	60	42	88	67

Underlined wavelengths are available in real lasers.

Gamut index for this set: $102 \leq R_g \leq 107$; R_g (average) = 103.8.

Gamut index R_g and the CIE 13.3 parameters were calculated after optimization.

(all < 40), indicating that certain colours will be very poorly rendered. In every case represented here, the worst performer was sample number (CES) 81 ($i = 81$) a dark purple-blue Type A sample⁴ (which represents a natural colour) (17).

Optimizing with TM–30–15

To do this, our optimization tool was modified in order to carry out calculations of R_f , $R_{f_{skin}}$ and $R_{f_{min}}$, using the new fitness function:

$$f_2 = aR_f + bR_{f_{min}} + cR_{f_{skin}} + d\eta \quad (5)$$

Note that we chose to include $R_{f_{skin}}$ as a component of Equation (5) as an indication of the acceptability of a spectrum for the illumination of social situations. As before, the weightings, a , b , c , d , were user-selectable, and the other symbols have the meanings defined previously. The differential evolution optimization engine operated as before. Note that the gamut index R_g was not included in the optimization process, and its value was instead computed after optimization was completed.

Fifty tests were run with a range of different weighting factors. As an aside, weight d was set to zero for the majority of runs since it was observed early on that the results gave $LER > 300$ lm/W irrespective and, any d greater than a small fraction caused the results to become dominated by LER at the expense of the colour properties. Sixteen results achieved $CCT > 2800$ K with $R_f \geq 85$; and a representative selection of ten is listed in Table 5. The majority of CCTs were in the 3000 K to 4000 K range, with two below 3000 K, and two above 4000 K. In all cases $R_g \geq 102$, $R_{f_{skin}} \geq 88$, and $R_{f_{min}} \geq 39$, as well as $R_f \geq 85$, and these data show some improvement on the TM–30–15 results of Table 4 – while the CIE 13.3 results suffer noticeable deterioration, particularly in terms of R_g . Three representative diagrams of SPDs from this set are given in Figure 2.

The CES (colour samples) identified as having the $R_{f_{min}}$ (lowest R_f results) show a greater spread than in Table 4. In order of decreasing frequency, they were numbers (17):

81 – dark purple-blue Type A sample (5/10)

42 – light olive green Type F sample (2/10)

37 – dark olive green Type A sample (1/10)

97 – dark pink-purple Type F sample (1/10)

98 – rich magenta Type A sample (1/10).

(Type A are of natural origin; Type F printed origin).

The wavelengths in Table 5 are also fairly well clustered around the averages, 452, 516, 570, 627 nm (which are about 5–10 nm higher than the Table 4 averages). Of the 40 individual wavelengths required in this instance, we have found only 5 that are currently available in solid-state laser products (510, 515, 520, 525 and 577 nm, with a total of 6 occurrences).

Figure 3 shows the LER-vs-CCT trends for the optimized spectra of Tables 3 and 4. Also plotted, for comparison, are the data for 136 commercial LED sources (17). For CCTs below 3000 K the simulated laser sources outperform the LEDs by margins of up to 100 lm/W, with the advantage reducing to roughly 50 lm/W at 4000 K, and some convergence evident above 5000 K.

Constrained optimisations

We have undertaken constrained optimizations with the intention of deriving mixtures of real (available) wavelengths with TM–30–15 properties at least as good as the Table 5 data.

The process was basically unchanged, except that there was a forced choice of wavelengths, utilizing a data library based on published lists of semiconductor lasers currently on the market. Each laser was again simulated by a (pseudo) delta function of 1-nm bandwidth. The programme was designed such that each run would select the four wavelengths whose mixture led to an optimized

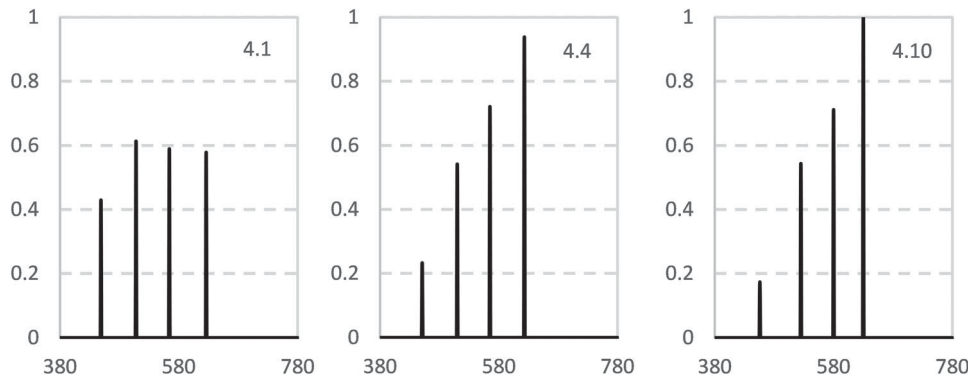


Figure 2. Relative spectral power distributions versus wavelengths (nm) for three of the Table 5 optimized spectra (identified by the SPD numbers in Table 5).

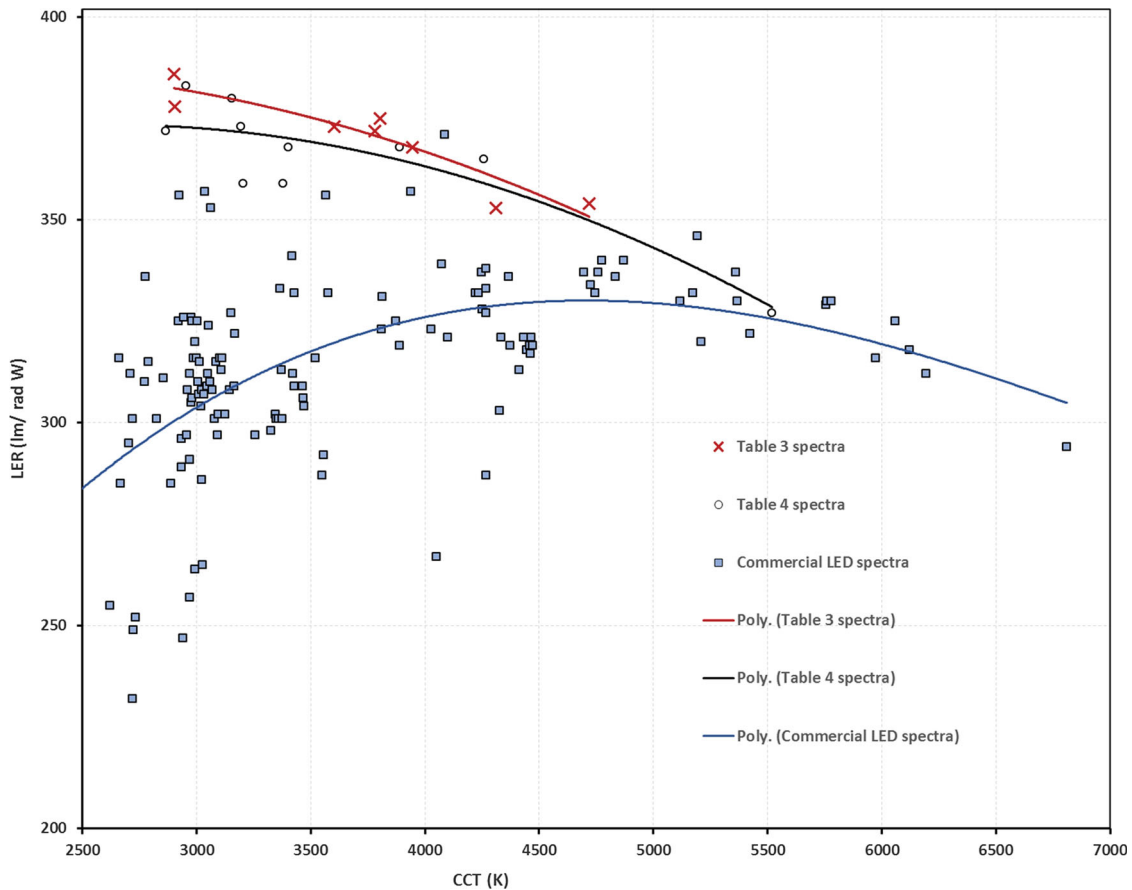


Figure 3. Luminous efficacy of radiation (LER) versus correlated colour temperature (CCT) for selected laser and LED sources. The curves are best-fit polynomials to each data set.

set of performance criteria based on the fitness function f_2 of Equation (5).

In order to keep the duration of each optimization run within reasonable bounds, the size of each data set was limited to 11 simulated lasers, with user-selected wavelengths spread approximately over the range of wavelengths discovered in the unconstrained optimizations. We created eight different 11-laser data sets, and ran

optimizations utilizing all eight sets. We collected data from over 100 optimization runs, and the more promising results are summarized in Tables 5 and 6.

These optimizations produced R_f results between 77 and 84. The most significant data for results having $R_f \geq 82$ are shown in Table 6. It appears that any increases in R_f are accompanied by reductions in the possible ranges of the other parameters listed.

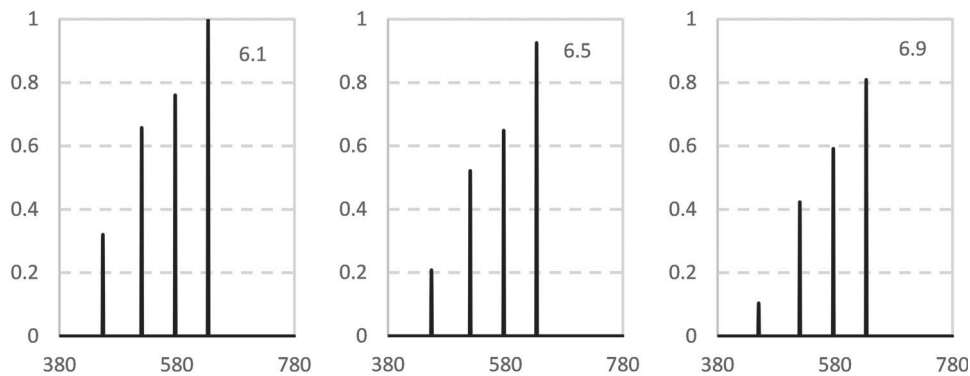
Table 6. Summary of results with $R_f \geq 82$. (Constrained optimizations using real laser wavelengths).

R_f	Number of results	$R_{f_{skin}}$ range		$R_{f_{min}}$ range		CCT range		LER range	
		min	max	min	max	(K)		(lm/W)	
						min	Max	min	max
82	26	80	94	45	61	2715	5527	301	371
83	11	83	90	47	61	2626	3619	314	370
84	9	87	91	58	63	3011	3593	344	364

NOTE: This table contains results using three different 11-laser data libraries.

Table 7. Details of spectra giving $R_f = 84$. (Constrained optimizations simulating real lasers).

SPD number	Wavelengths nanometres				CCT (K)	CIE (u', v') co-ord's	LER (lm/W)	TM-30-15					CIE 13.3	
								R_f	R_g	$R_{f_{skin}}$	$R_{f_{min}}$	i_{min}	R_a	R_9
6.1	454	520	577	633	3593	0.230, 0.520	349	84	106	89	58	20	85	32
6.2	454	520	577	633	3568	0.228, 0.527	357	84	104	87	61	40	85	38
6.3	454	520	577	633	3338	0.236, 0.528	356	84	104	88	62	97	85	38
6.4	454	520	577	633	3261	0.239, 0.528	352	84	105	89	62	97	85	31
6.5	454	520	577	633	3240	0.239, 0.528	350	84	105	89	63	20	85	25
6.6	454	520	577	633	3103	0.244, 0.532	351	84	104	89	62	97	85	26
6.7	454	520	577	633	3047	0.246, 0.531	347	84	106	90	62	63	85	19
6.8	454	520	577	633	3014	0.248, 0.529	344	84	107	91	61	20	85	17
6.9	<u>450</u>	520	577	633	3011	0.245, 0.540	364	84	100	87	59	97	83	46

**Figure 4.** Relative spectral power distributions versus wavelengths (nm) for three of the Table 7 optimized spectra (identified by the SPD numbers in Table 7).

Details of the nine cases for which we obtained $R_f = 84$ are given in Table 7, and three representative SPDs from this set are given in Figure 4. As noted above, they exhibit narrow ranges of the key TM-30-15 parameters; and the reason becomes evident when one studies the wavelengths in the mixtures – i.e. an almost consistent set of identical wavelengths, with only SPD 6.9 differing in respect of its shortest component wavelength.

In terms of lighting system design criteria, the range of CCTs derived here is relatively narrow. However, it is a reasonably significant range (54 MK^{-1}).

The CIE 13.3 properties of these spectra are rather poor – particularly the low values for R_9 (≤ 46). These need to be weighed against the reasonably good skin rendition ($R_{f_{skin}}$) and minima ($R_{f_{min}}$) in the R_f domain. As before, the i_{min} term lists the colour sample identified as having the lowest R_f result ($R_{f_{min}}$) in each instance. In

order of decreasing frequency, they were CES numbers (17):

- 97 – dark pink-purple Type F sample (4/9)
- 20 – dark orange Type F sample (3/9)
- 63 – moderate grey Type F sample (1/9)
- 40 – dark olive/brown Type F sample (1/9).

(Note: Type F samples derive from printed materials)

Conclusions

We have demonstrated that it will very likely be possible in the future to produce high-intensity light sources based on mixtures of four lasers. These sources will have high conversion efficiency and high luminous efficacy (Figure 3) coupled with very acceptable (although not outstanding) colour properties. The fact that $R_{f_{min}}$ in our experiments has been associated mainly with moderately

dark colours is an indication that many colours in everyday experience will be satisfactorily rendered by our optimized laser mixtures. Of course, this can also indicate unsatisfactory colour rendition in critical situations.

The range of colour temperatures is somewhat limited if the highest R_f (84 in Table 7) is desired. However, the CCT range is a great deal broader if a slightly lower R_f is acceptable (Table 6). In certain cases this may also entail trade-offs in terms of other parameters such as LER or $R_{f_{skin}}$ or $R_{f_{min}}$.

Our unconstrained results (Table 5) indicate further possible improvements in both R_f and LER (and other performance measures) provided that lasers of the appropriate wavelengths can be developed (and perhaps this paper will can provide the stimulus for this).

Table 4 shows that unconstrained optimization in terms of CIE 13.3 parameters can produce excellent R_a and R_9 performance, coupled with good R_f and $R_{f_{skin}}$ properties – but at the expense of exceptionally poor $R_{f_{min}}$ results, which indicates a high likelihood of unsatisfactory lighting conditions, and which supports the caveats (7,11) noted earlier.

Our examination of the work of Neumann et al. (13), and simulation of their published spectra, indicates a highest probable value for R_f of 82 (at their two lower colour temperatures). These were rated in their paper as equivalent to high-quality reference illuminants; and we therefore deduce that our optimized spectra scoring $R_f \geq 83$ would also be so categorized. Another notable feature of their results was the drop in R_f values for the higher CCTs – something also reflected in our Table 6.

Finally, we need to note that the aim here has been to establish the feasibility of optimizing laser mixtures as white-light sources, but it is recognized that several other issues will have to be taken into consideration in practice.

As noted in Table 1, the chief optical requirement is to eliminate the undesirable effects of speckle and coloured shadows, which can be overcome by the use of diffusers to assist the mixing process and to remove speckle.

We also note that it will be essential to allay safety concerns by ensuring that adequate de-coherence of high-power laser beams is achieved.

Table 1 also alluded to the increased complexity of the electronics control requirements – in addition to which it is recognized that all laser lighting systems will need to include sophisticated heat-sinking designs.

Developments in this area are at present constrained by the need for complex and costly electronic and optical design, development, and test systems. It is hoped that these limitations can be overcome once the potential benefits of laser lighting are accepted by the global semiconductor and lighting manufacturing industries.

Notes

1. Not to be confused with the overall luminous efficacy which compares the visible light output against the electrical power consumed, which necessarily takes account of the conversion efficiency of the device (electrical to radiant watts).
2. A useful visualization tool for the CIE coordinate systems can be found on the internet at: <http://www.efg2.com/Lab/Graphics/Colors/Chromaticity.htm>.
3. The interested reader may wish to compare the 2 MK^{-1} here with the 54 MK^{-1} derived from Table 7.
4. In this and subsequent sections of the paper, we have used our own interpretations to describe the TM–30–15 sample colours.

Acknowledgements

This work was supported by the School of Professional Engineering and the Manukau Institute of Technology Research Fund.

The second author thanks Professor Ahmed Al-Jumaily, director of IBTec at AUT, for his support and the provision of facilities.

The authors acknowledge the IES TM–30–15 spreadsheet (17) as the source of the 136 LED spectra whose performance is plotted in Figure 3.

Disclosure statement

No potential conflict of interest was reported by the authors.

Funding

This work was supported by Manukau Institute of Technology Research Fund.

References

- (1) Commission Internationale de l'Eclairage. *Method of Measuring and Specifying Colour Rendering Properties of Light Sources*; CIE Publication 13.3, CIE: Vienna, **1995**.
- (2) Fumagalli, S.; Bonanomi, C.; Rizzi, A. Experimental Assessment of Color-Rendering Indices and Color Appearance Under Varying Setups. *J. Mod. Optic.* **2015**, *62* (1), 56–66.
- (3) Davis, W.; Ohno, Y. Color Quality Scale. *Opt. Eng.* **2010**, *49* (3), 033602.
- (4) Illuminating Engineering Society of North America. *IES Method for Evaluating Light Source Color Rendition*; Illuminating Engineering Society: New York, **2015**.
- (5) David, A.; Fini, P.T.; Houser, K.W.; Ohno, Y.; Royer, M.P.; Smet, K.A.G.; Wei, M.; Whitehead, L. Development of the IES Method for Evaluating the Color Rendition of Light Sources. *Opt. Express* **2015**, *23* (12), 15888–15906.
- (6) Royer, M.P.; Wei, M. The Role of Presented Objects in Deriving Color Preference Criteria From Psychophysical Studies. *LEUKOS* **2017**, *13* (3), 143–157.
- (7) Smet, K.A.G.; David, A.; Whitehead, L. Why Color Space Uniformity and Sample set Spectral Uniformity are Essential for Color Rendering Measures. *LEUKOS* **2016**, *12*, 1–2. 39–50.

- (8) Wyszecki, G.; Stiles, W.S. *Color Science: Concepts and Methods, Quantitative Data and Formulae*, 2nd ed.; Wiley: New York, **1982**.
- (9) Commission Internationale de l'Éclairage. *Colorimetry*, 3rd ed.; CIE Publication 15.3, CIE: Vienna, **2003**.
- (10) S. Soltic; Chalmers, A.N. Optimization of Laser-Based White Light Illuminants. *Opt. Express*. **2013**, *21* (7), 8964–8971.
- (11) David, A. Color Fidelity of Light Sources Evaluated Over Large Sets of Reflectance Samples. *LEUKOS* **2014**, *10* (2), 59–75.
- (12) Coltrin, M.E.; Tsao, J.Y.; Ohno, Y. Limits on the Maximum Attainable Efficiency for Solid-State Lighting. Proc. SPIE 6841, 684102–1–684102–12, 2007.
- (13) Neumann, A.; Wierer, J.J., Jr.; Davis, W.; Ohno, Y.; Brueck, S.R.J.; Tsao, J.Y. Four-color Laser White Illuminant Demonstrating High Color-Rendering Quality. *Opt. Express* **2011**, *19* (S4 Suppl 4), A982–A990.
- (14) Schiller, D. Beyond LED. *enLIGHTenment Magazine* **Jan 2014**, 132–136.
- (15) Ledru, G.; Catalano, C.; Dupuis, P.; Zissis, G. Efficiency and Stability of a Phosphor-Conversion White Light Source Using a Blue Laser Diode. *AIP Adv.* **2014**, *4* (10), 107134.
- (16) Diode-pumped solid-state laser [Online], http://en.wikipedia.org/wiki/Diode-pumped_solid-state_laser (accessed Dec 12, 2017).
- (17) Official version of Excel worksheet, available with purchase of the IES TM–30–15 Technical Memorandum, downloaded from <http://www.ies.org/redirect/tm-30/> (accessed Nov 20, 2015).
- (18) Soltic, S.; Chalmers, A.N. Differential Evolution for the Optimisation of Multi-Band White LED Light Sources. *Lighting Res. Tech.* **2011**, *0*, 1–14.